Journal of Chemical Neuroanatomy 126 (2022) 102168

Contents lists available at ScienceDirect

Journal of Chemical Neuroanatomy

journal homepage: www.elsevier.com/locate/jchemneu

Effects of 3.5 GHz radiofrequency radiation on ghrelin, nesfatin-1, and irisin level in diabetic and healthy brains

Hava Bektas [a], Sermin Algul [b], Fikret Altindag [c], Korkut Yegin [d], Mehmet Zulkuf Akdag [e], Suleyman Dasdag [f,*]

[a] Department of Biophysics, Medical School of Van Yuzuncu Yil University, Van, Turkey
[b] Department of Physiology, Medical School of Van Yuzuncu Yil University, Van, Turkey
[c] Department of Histology and Embryology, Medical School of Van Yuzuncu Yil University, Van, Turkey
[d] Department of Electrical and Electronics Engineering, Faculty of Engineering, Ege University, Turkey
[e] Department of Biophysics, Medical School of Dicle University, Diyarbakır, Turkey
[f] Department of Biophysics, Medical School of Istanbul Medeniyet University, Istanbul, Turkey

ARTICLE INFO

Keywords:
Radiofrequency radiation
Diabetes
Brain
Ghrelin
Nesfatin-1
Irisin

ABSTRACT

Diabetes, mobile phone use, and obesity have increased simultaneously in recent years. The radiofrequency radiation (RFR) emitted from mobile phones is largely absorbed in the heads of users. With 5 G, which has started to be used in some countries without the necessary precautions being taken, the amount of RFR to which living things are exposed will increase. In this study, the changes in energy homeostasis and redox balance caused by 5 G (3.5 GHz, GSM-modulated) were explored. The effects of RFR on the brains of diabetic and healthy rats were investigated and histopathological analysis was performed. Twenty-eight Wistar albino rats weighing 200–250 g were divided into 4 groups as sham, RFR, diabetes, and RFR+diabetes groups (n = 7). The rats in each group were kept in a plexiglass carousel for 2 h a day for 30 days. While the rats in the experimental groups were exposed to RFR for 2 h a day, the rats in the sham group were kept under the same experimental conditions but with the radiofrequency generator turned off. At the end of the experiment, brain tissues were collected from euthanized rats. Total antioxidant (TAS), total oxidant (TOS), hydrogen peroxide (H_2O_2), ghrelin, nesfatin-1, and irisin levels were determined. In addition, histopathological analyses of the brain tissues were performed. The specific absorption rate in the gray matter of the brain was calculated as 323 mW/kg and 195 mW/kg for 1 g and 10 g averaging, respectively. After RFR exposure among diabetic and healthy rats, decreased TAS levels and increased TOS and H_2O_2 levels were observed in brain tissues. RFR caused increases in ghrelin and irisin and a decrease in nesfatin-1 in the brain. It was also observed that RFR increased the number of degenerated neurons in the hippocampus. Our results indicate that 3.5 GHz RFR causes changes in the energy metabolism and appetite of both healthy and diabetic rats. Thus, 5 G may not be innocent in terms of its biological effects, especially in the presence of diabetes.

1. Introduction

Rapid developments in wireless communication technologies, especially mobile phones, and the intensive use of these instruments by people of all ages have led scientists to focus their attention on the human health effects of the radiofrequency radiation (RFR) emitted by these technologies. While 2 G, 3 G, 4 G, and 4.5 G technologies use radiofrequency waves of 900 MHz, 1800 MHz, and 2100 MHz, the most preferred radiofrequency band for 5 G technology, which has begun to be used in many countries in recent years, is 3.5 GHz (Dasgupta et al., 2020; Wang et al., 2022). With the innovations offered by 5 G technology and the application of the internet of things, the RFR exposure time and intensity of living things are increasing. The RFR emitted from mobile phones is not sufficient for the ionization of molecules and the activation of orbital electrons. It is now known that the underlying mechanism of DNA and other cellular elements affected by RFR is oxidative stress (Dasdag and Akdag, 2016; Yakymenko et al., 2016). It has been suggested that RFR (2.45 GHz, with 217 Hz pulses, during 60 min/day for 30 days, whole-body SAR 0.1 W/kg) can change cation transitions by affecting voltage-dependent channels in DRG neurons and

* Correspondence to: Suleyman Dasdag Department of Biophysics, Medical School of Istanbul Medeniyet University, 34700 Uskudar, Istanbul, Turkey.
E-mail address: sdasdag@gmail.com (S. Dasdag).

https://doi.org/10.1016/j.jchemneu.2022.102168
Received 17 June 2022; Received in revised form 4 October 2022; Accepted 4 October 2022
Available online 8 October 2022
0891-0618/© 2022 Elsevier B.V. All rights reserved.

brains of Wistar Albino rats (Nazıroğlu et al., 2012). The use of 5 G with other currently used generations of technology standards with different frequencies will lead to accumulative effects (Tan et al., 2017). Cumulative biological effects are strongly related to the intensity and duration of radiofrequency exposure. The current exposure limits are based on adverse health outcomes due to temperature rise (tissue warming and inducible tissue stimulation from short-term or acute exposures) (Belpomme et al., 2018). There are no precautions for chronic and/or cumulative health risks associated with radiofrequency energy at substandard levels (Dolan and Rowley, 2009). Changes mediated by reactive oxygen species (ROS) are the most convincing mechanisms put forward to explain the effects of RFR on living things (Dasdag and Akdag, 2016; Yakymenko et al., 2016). Because the brain, a vital organ, is particularly close to the source of RFR exposure, studies on the effects of RFR have mostly focused on the brain and the brain was shown to be affected by RFR (Kim et al., 2021; Tripathi et al., 2021). In addition, brain tissues are more vulnerable to oxidative damage due to their low levels of antioxidant enzyme activity and high oxygen consumption (Motawi et al., 2014). There are a number of studies reporting that exposure to RFR at various specific absorption rate (SAR) levels causes oxidative stress in the brain (Avci et al., 2012; Chauhan et al., 2017; Chen et al., 2011; Kesari et al., 2011; Shehu et al., 2016; Singh et al., 2020). Other studies have revealed that the basis of age-related neurodegenerative diseases is imbalance in redox mechanisms (Sahin et al., 2016).

Diabetes mellitus (DM) is a disease that is spreading rapidly around the world due to the living conditions of people today and it carries with it high risks of mortality and morbidity. Studies reported that ROS and lipid peroxidation are significantly increased in rats with experimentally induced diabetes and in human patients with diabetes, and oxidative stress has a role in the etiology and progression of diabetes (Wang et al., 2018). DM is associated with increased ROS production, inadequate antioxidant defense mechanisms, and, consequently, increased oxidative stress (Bathina and Das, 2021).

Studies on mediators that have effects on nutrition in humans and animals have led researchers to focus on nesfatin and ghrelin. These are hormones that influence food intake, while irisin is one of the hormones that are effective in regulating energy metabolism (Price et al., 2007). It is accepted that appetite is controlled by the brain and eating is regulated by complex mechanisms in the central nervous system and particularly in the hypothalamus (Druce and Bloom, 2003). The level of ghrelin is increased by fasting and it decreases within 60–120 min following food intake (Tschop et al., 2001). In rats, it was shown that fasting increased ghrelin release, while carbohydrate intake decreased ghrelin release (Cummings et al., 2001). It is thought that adipose tissue and appetite-enhancing effects of ghrelin are regulated by special neurons in the central nervous system (Tschop et al., 2001).

It is known that nesfatin plays roles in the brain not only in the regulation of food intake but also in the regulation of some brain functions, autonomic regulation, stress, mood, and REM sleep (Jego et al., 2012).

Irisin is a hormone attracting the attention of researchers since its recent discovery; it is thought to have potential in the treatment of many metabolic diseases in the future, especially obesity and diabetes, and it is a highly effective peptide in neurodegeneration (Moreno-Navarrete et al., 2013).

In a recent human study, 15 normal-weight young individuals (23.47 ± 0.68 years) were exposed to sham radiation and two different types of mobile phones emitting 900 MHz RFR (0.97 W/kg and 1.33 W/kg) under fasting conditions for 25 min. Afterwards, spontaneous food intake was determined by an ad libitum standard buffet test and cerebral energy homeostasis was monitored by phosphorus-magnetic resonance spectroscopy measurements. It was reported that exposure to both types of mobile phones strikingly increased the overall caloric intake by 22–27 % compared to the sham condition (Wardzinski et al., 2022). Moreover, measurement results of cerebral energy contents, such as the ratios of adenosine triphosphate and phosphocreatine to inorganic phosphate, showed increases with cell phone radiation exposure (Wardzinski et al., 2022). These researchers argued that RFR is a potential contributor to the overeating that underlies the obesity epidemic (Wardzinski et al., 2022). Furthermore, pulsed and amplitude modulated microwaves were shown to affect brain energy homeostasis in rats (Sanders et al., 1985). It was also demonstrated that both the brain and energy homeostasis are affected by RFR (Tripathi et al., 2021). Based on these previous findings, we hypothesized that 3.5 GHz RFR exposure affects irisin, ghrelin, and nesfatin-1 levels via oxidant and antioxidant redox systems in the brain.

The present study was designed to determine the effects of exposure to 3.5 GHz RFR (GSM, 217 Hz modulation frequency, pulse width 577 μs) emitted from 5 G technologies on total antioxidant (TAS), total oxidant (TOS), hydrogen peroxide (H_2O_2), nesfatin, ghrelin, and irisin levels in the brains of healthy and diabetic rats and possible histological changes.

2. Materials and methods

2.1. Animal care

This experimental study was carried out in the Experimental Research and Application Center of Van Yuzuncu Yil University. All stages of the study were designed and performed according to the guidelines of the Animal Experiments Local Ethics Committee of Van Yuzuncu Yil University (Protocol No: 2021/05–10).

A total of 28 healthy male Wistar albino rats (8–10 weeks old and weighing 200–250 g) were obtained from the Experimental Animal Research Center of Van Yuzuncu Yil University. The rats were separated and placed in four stainless steel cages with seven rats per cage and were maintained with a 12-hour dark/light cycle. Rats were allowed free access to pellet feed (Purina, Istanbul, Turkey) containing 21 % crude protein and daily drinking water ad libitum in optimal environmental conditions (22 ± 2 °C and 60 ± 5 % humidity).

2.2. Animal grouping and protocol

This study included four different groups of rats (n = 7 for each group). In Group 1 (healthy sham group), healthy rats (n = 7) were kept in a plexiglass carousel for 2 h a day for 30 days while the radiofrequency generator was turned off. In Group 2 (healthy RFR group), healthy rats (n = 7) were irradiated with radiofrequency signals (3.5 GHz, GSM-modulated) in the plexiglass carousel for 2 h a day for 30 days. In Group 3 (diabetes sham group), rats with diabetes were kept in the plexiglass carousel for 2 h a day for 30 days while the generator was turned off. In Group 4 (RFR+diabetes group), rats with diabetes were irradiated with RFR (3.5 GHz, GSM-modulated) for 2 h a day for 30 days (n = 7).

2.3. Induction of experimental diabetes

Streptozotocin (STZ) is an antibiotic that produces pancreatic islet β-cell destruction and is widely used experimentally to produce models of type 1 DM (Furman, 2015). To induce experimental diabetes, rats in Groups 3 and 4 were fasted overnight and then 45 mg/kg of STZ was administered intraperitoneally in a single dose. Blood samples were taken from rats 72 h after STZ application to confirm the presence of DM. Blood glucose levels were measured by a glucometer (IME-DC) and blood glucose levels above 250 mg/dL were considered as diabetic (Öntürk and Özbek, 2007).

2.4. Exposure and field measurements

A GSM signal generator (3500 PM10 model, Everest Comp., Adapazari, Turkey) that produces a 3500 MHz band (GSM-modulated) radiofrequency waveform identical to that of mobile phones was used in

this study to expose the rats to RFR. The emitted power (omnidirectional on the plane perpendicular to the antenna axis) of the generator was fixed during exposure. The antenna of the generator was equivalent to that of a typical mobile phone. Rats were confined in a plexiglass carousel and exposed to 3500 MHz RFR emitted from the generator. The carousel was surrounded with electromagnetic absorber material backed by metal to isolate outdoor electromagnetic fields from the test setup during the study duration of 1 month. Power density and the electrical field were measured with a TES 593 field probe (Shenzhen, Guangdong, China). The measured electric field and power density values were 28.1 V/m, 1.6 W/m^2. The rats in the exposure groups were exposed to RFR for 2 h per day (5 days a week) for 1 month. For the sham groups, rats were placed in the carousel and the same procedure was applied except that the generator was turned off, i.e., no radiofrequency signal was present. The antenna of the generator was placed at the center of the plexiglass carousel to provide ideal exposure conditions. The distance of the antenna from the heads of the rats was 1 cm (Alkis et al., 2019). All rats were kept under identical conditions for 1 month with free access to food and water. The experimental setup is illustrated in Fig. 1.

2.5. Specific absorption rate (SAR) analysis

The simulation setup was created to match the experimental setup as much as possible. The applicator antenna, the Faraday cage, and the rats were all modeled in a 3D electromagnetic field solver using CST (CST AG, Darmstadt, Germany) (Alkis et al., 2019). The simulation model is depicted in Fig. 1. An accurate rat model based on computerized tomography scans is readily available for biological CST applications. This rat voxel (volumetric pixel) model is very detailed and includes all tissues within the rat. While peak power of 2 W is common for GSM burst signals, average power for SAR evaluations is taken as 250 mW. Electromagnetic and thermal modeling within CST is based on the finite-integration technique, which is a combined method of integral and differential solvers acting in space and time, respectively. Simulated electric field values were also compared to measured field values with the TES 593 field probe to validate the simulation setup.

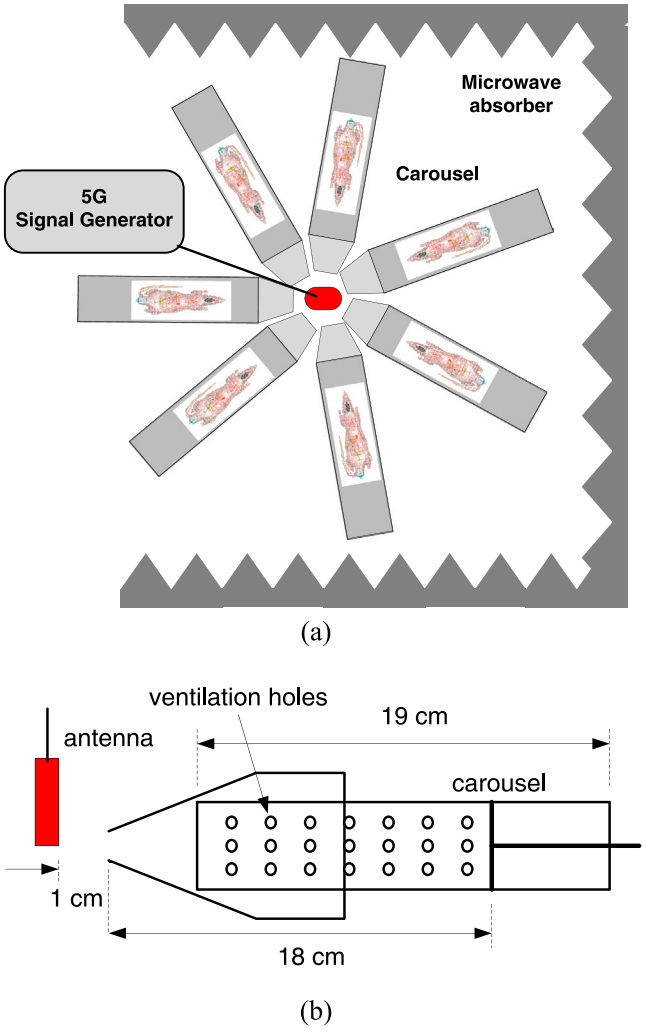


Fig. 1. Experimental setup: a) exposure setup, b) plexiglass carousel and antenna.

2.6. Sample collection and preparation of brain tissue homogenates

At the end of the experiment, under ketamine (Ketasol, Richter Pharma AG, Vienna, Austria) and bacillazine (Rompin, Istanbul, Turkey) anesthesia, the rats were killed by cervical dislocation and the brains were removed immediately. Part of the brain was used for the preparation of a homogenate. The brain tissues were carefully washed and weights were recorded. The 10 % homogenate was prepared in phosphate-buffered saline (PBS) and centrifuged at 10,000g for 10 min. The supernatant was collected for further biochemical assays. Supernatants from brain homogenates were not frozen and analyzed immediately after the study.

2.7. Nesfatin-1 analyses

The kit used in this study is a sandwich enzyme immunoassay for the in vitro quantitative measurement of nesfatin-1 (SunRed Biological Technology Co., Ltd., Shanghai, China, Catalog No: 201-11-1426). Each well of the supplied microtiter plate is precoated with a target-specific capture antibody. Standards and samples are added to the wells and the target antigen binds to the NES-1 antibody labeled with biotin. Afterwards, a streptavidin-HRP conjugate, chromogen A and B substrate, and stop solution are added to terminate color development reactions and then the optical density of the wells is measured at a wavelength of 450 ± 2 nm using automated optical densitometry (intra-assay CV: <8 %, inter-assay CV: <11 %, sensitivity: 28.951 ng/L, assay range: 30–9000 ng/L). Each sample was run in duplicate and the mean value was used for analysis. This assay has high sensitivity and excellent specificity for detection of rat nesfatin-1. No significant cross-reactivity or interference between rat nesfatin-1 and analogues was observed (Algul et al., 2021).

2.8. Ghrelin analysis

The kit used in this study is a sandwich enzyme immunoassay for the in vitro quantitative measurement of ghrelin (SunRed Biological Technology Co., Ltd., Shanghai, China, Catalog No: 201-11-1650). Each well of the supplied microtiter plate is precoated with a target-specific capture antibody. Standards and samples are added to the wells and the target antigen binds to the ghrelin antibody labeled with biotin. Afterwards, a streptavidin-HRP conjugate, chromogen A and B substrate, and stop solution are added to terminate color development reactions and then the optical density of the wells is measured at a wavelength of 450 ± 2 nm using automated optical densitometry (sensitivity: 38.572 pg/mL, assay range: 40–10000 pg/mL). Each sample was run in duplicate and the mean value was used for analysis. This assay has high sensitivity and excellent specificity for detection of rat ghrelin. No significant cross-reactivity or interference between rat ghrelin and analogues was observed (Kızılırmak et al., 2020).

2.9. Irisin analysis

The kit used in this study is a sandwich enzyme immunoassay for the

in vitro quantitative measurement of irisin (SunRed Biological Technology Co., Ltd., Shanghai, China, Catalog No: 201-11-1713). Each well of the supplied microtiter plate is precoated with a target-specific capture antibody. Standards and samples are added to the wells and the target antigen binds to the irisin antibody labeled with biotin. Afterwards, a streptavidin-HRP conjugate, chromogen A and B substrate, and stop solution are added to terminate color development reactions and then the optical density of the well is measured at a wavelength of 450 ± 2 nm using automated optical densitometry (sensitivity: 0.247 ng/mL, assay range: 0.3–90 ng/mL). Each sample was run in duplicate and the mean value was used for analysis. This assay has high sensitivity and excellent specificity for detection of rat irisin. No significant cross-reactivity or interference between rat irisin and analogues was observed (Akdag and Odabas, 2020).

2.10. Total antioxidant status (TAS) analysis

The kit used in this study is a sandwich enzyme immunoassay for the in vitro quantitative measurement of TAS (SunRed Biological Technology Co., Ltd., Shanghai, China, Catalog No: 201-11-2672). Each well of the supplied microtiter plate is precoated with a target-specific capture antibody. Standards and samples are added to the wells and the target antigen binds to the TAS antibody labeled with biotin. Afterwards, a streptavidin-HRP conjugate, chromogen A and B substrate, and stop solution are added to terminate color development reactions and then the optical density of the wells is measured at a wavelength of 450 ± 2 nm using automated optical densitometry (intra-assay CV: <9 %, inter-assay CV: <11 %, sensitivity: 0.175 U/mL, assay range: 0.2–60 U/mL). Each sample was run in duplicate and the mean value was used for analysis. The sensitivity and specificity of assay for detection of rat TAS is in acceptable ranges.

2.11. Total oxidant status (TOS) analysis

The kit used in this study is a sandwich enzyme immunoassay for the in vitro quantitative measurement of TOS (SunRed Biological Technology Co., Ltd., Shanghai, China, Catalog No: 201-11-1669). Each well of the supplied microtiter plate is precoated with a target-specific capture antibody. Standards and samples are added to the wells and the target antigen binds to the TOS antibody labeled with biotin. Afterwards, a streptavidin-HRP conjugate, chromogen A and B substrate, and stop solution are added to terminate color development reactions and then the optical density of the wells is measured at a wavelength of 450 ± 2 nm using automated optical densitometry (intra-assay CV: <8 %, inter-assay CV: <10 %, sensitivity: 0.073 nmol/mL, assay range: 0.1–20 nmol/mL). Each sample was run in duplicate and the mean value was used for analysis. The sensitivity and specificity of assay for detection of rat TOS is in acceptable ranges.

2.12. H_2O_2 analysis

The kit used in this study is a sandwich enzyme immunoassay for the in vitro quantitative measurement of H_2O_2 (SunRed Biological Technology Co., Ltd., Shanghai, China, Catalog No: 201-11-3366). Each well of the supplied microtiter plate is precoated with a target-specific capture antibody. Standards and samples are added to the wells and the target antigen binds to the H_2O_2 antibody labeled with biotin. Afterwards, a streptavidin-HRP conjugate, chromogen A and B substrate, and stop solution are added to terminate color development reactions and then the optical density of the wells is measured at a wavelength of 450 ± 2 nm using automated optical densitometry (sensitivity: 9.005 ng/mL, assay range: 10–3000 ng/mL). Each sample was run in duplicate and the mean value was used for analysis. This assay has high sensitivity and excellent specificity for detection of rat H_2O_2. No significant cross-reactivity or interference between rat H_2O_2 and analogues was observed (Kamiş and Karabağ, 2019).

2.13. Immunohistochemical staining

After another part of the brain was fixed in 10 % buffered formaldehyde, the samples were embedded in paraffin following routine histological processing steps. Sections of 4 μm in thickness were taken from paraffin blocks with a microtome and placed on lysine slides. Sections were deparaffinized and rehydrated, and then incubated in 3 % H_2O_2 for 10 min to prevent endogenous peroxidase enzyme activity. To prevent antigen masking in the nucleus, they were heated in antigen retrieval solution (citrate buffer, pH 6.1) in a microwave oven twice. Then, to prevent nonspecific binding, the protein block was dropped and incubated for 10 min. Anti-synaptophysin antibody (Santa Cruz Biotechnology, sc-365447, dilution: 1/100) was used as the primary antibody. After adding the antibody, these samples were incubated in a humidity chamber at 4 °C for one night. After rinsing with PBS, biotinylated goat anti-polyvalent and streptavidin-peroxidase conjugate were dropped and incubated for 10 min, respectively. After the application of diaminobenzidine (DAB), used as a chromogen, samples were stained with Mayer's hematoxylin and examined under a light microscope (Olympus BX53, Olympus, Japan) (Altındağ et al., 2021). Immunohistochemical findings were assessed as negative (-), slightly positive (+), moderately positive (++), and intensely positive (+++) according to the immunostaining characteristics of the cells.

2.14. Cresyl violet staining method

To evaluate neuronal damage in the hippocampus of rats exposed to 5 G and induced diabetes, the 0.1 % cresyl violet staining method, which specifically stains Nissl bodies, was applied. Brain sections taken at 5 μm in thickness were deparaffinized, dehydrated, and stained with cresyl violet for 30 min. Neurons stained with cresyl violet were evaluated and photographed by a blinded histologist under a light microscope (Olympus BX53, Olympus, Japan) according to low and high staining intensity (Jin and Bo, 2021; Justin et al., 2018; Tóthová et al., 2018).

2.15. Statistical analysis

The SPSS statistical software program was used in the analyses. Whether the data of each group originated from the same distribution was tested by rank-based Kruskal-Wallis tests or one-way ANOVA. For comparisons of groups, the Mann-Whitney test was used to determine if there was a statistically significant difference between them. The results were presented as medians and $p < 0.05$ was taken to be statistically significant. In tables, the groups were labeled with letters to indicate differences such that if a group has a different letter than others a statistically significant difference exists.

3. Results

3.1. Results of body weight

While the average initial weight of the healthy rats was 233.5 g, it was increased to 302.5 g at the end of the RFR exposure ($p = 0.004$).

Table 1
Body weights of the rats.

Groups	Weight (g)	p
Healthy sham (start)	237.5 ± 21.9[a]	0.128
Healthy sham (end)	261 ± 25.4[a]	
Healthy RFR (start)	233.5 ± 11.2[a]	0.004
Healthy RFR (end)	302.5 ± 113.8[b]	
Diabetes sham (start)	281.5 ± 8.12[a]	0.045
Diabetes sham (end)	254 ± 26.1[b]	
Diabetes RFR (start)	267.5 ± 18.1[a]	0.055
Diabetes RFR (end)	249 ± 21.7[a]	

[a,b]:Different letters indicate significant differences between groups.

There was no significant change in the weights of the diabetic rats after 5 G exposure (Table 1).

3.2. SAR results

SAR calculations based on the IEEE/IEC 62704-1 method were used to evaluate the SAR distribution. Whole-body SAR was found to be 37 mW/kg. SAR of the gray matter of the brain was calculated as 323 mW/kg and 195 mW/kg for 1 g and 10 g averaging, respectively. The maximum SAR of the blood and blood vessels was 162 mW/kg and 178 mW/kg for 1 g and 10 g averaging, respectively. In fat tissues, SAR reached maximum values of 220 mW/kg and 184 mW/kg for 1 g and 10 g averaging, respectively. The rat voxel model, rat brain, blood vessels, and blood are shown in Fig. 2. SAR distributions for 1 g and 10 g averaging on different cut-planes are displayed in Fig. 3.

3.3. ELISA results

There was a significant difference between the groups for levels of ghrelin in the brain ($p = 0.001$). Ghrelin levels in the brain were increased in Group 2 compared to Group 1 and in Group 4 compared to Group 3 (Table 2).

There was a significant difference between the groups in nesfatin-1 levels in the brain ($p = 0.018$). Nesfatin-1 levels in the brain were decreased in Group 2 compared to Group 1 and in Group 4 compared to Group 3 (Table 2).

There was a significant difference between the groups in the level of irisin in the brain ($p = 0.001$). Irisin levels in the brain were decreased in Group 2 compared to Group 1 and in Group 4 compared to Groups 1 and 2 (Table 2).

There was a significant difference between the groups in the TAS of the brain ($p = 0.002$). TAS values of the brain were decreased in Group 2 compared to Group 1 and in Group 4 compared to Group 3 (Table 2).

There was a significant difference between the groups in the TOS of the brain ($p < 0.001$). TOS values of the brain were increased in Group 2 compared to Group 1 and in Group 4 compared to Group 3 (Table 2).

There was a significant difference between the groups in the level of H_2O_2 in the brain ($p < 0.001$)·H_2O_2 levels in the brain were increased in Group 2 compared to Group 1 and in Group 4 compared to Group 3 (Table 2).

There was no difference between the groups in terms of anti-synaptophysin expression (Fig. 4).

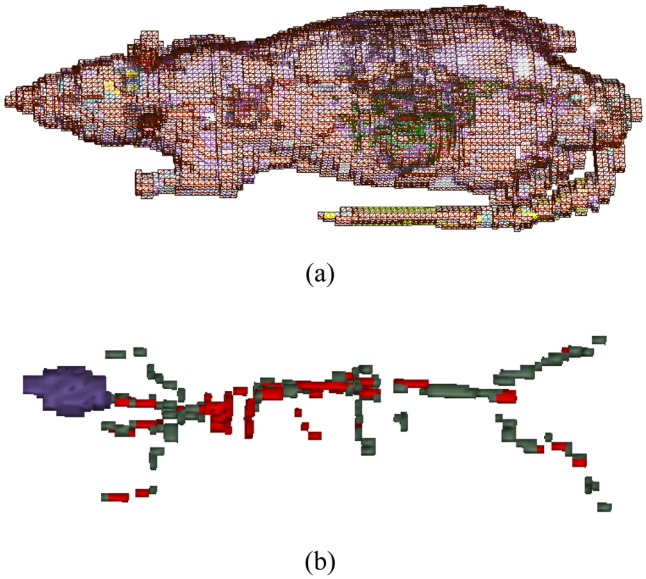


Fig. 2. a) Rat voxel model; b) gray matter, blood and blood vessels.

The intensity of cresyl violet staining, which we performed to evaluate the intensity of neuronal degeneration, was lower in Group 1. High cresyl violet staining intensity was found in Groups 2, 3, and 4, and it was particularly intense in Group 2 (Fig. 5).

4. Discussion

There is growing concern about increasing electromagnetic pollution due to RFR emitted from wireless devices. Exposure to RFR varies from individual to individual according to the length of time and frequency of use of such devices. The 3.5 GHz band is one of the frequency bands used in 5 G technology (Dasgupta et al., 2020; Wang et al., 2022) and it was consequently selected for the present study. Older wireless telephones use frequencies in the 900, 1800, and 2100 MHz ranges. The mechanisms induced by RFR remain unknown, but commonly accepted theories include changes in membrane permeability and ROS production (Nazıroğlu et al., 2012).

The results of the present study showed that 3.5 GHz RFR caused a significant increase in TOS and H_2O_2 and a decrease in TAS in healthy rats, and these changes were more intense in the brains of diabetic rats. Our findings are in agreement with the results of previous studies that demonstrated RFR-induced oxidative stress in the brain (Chen et al., 2011; Ertilav et al., 2018) due to its polyunsaturated fatty acid-rich composition and high metabolic rate (Singh et al., 2020). Supporting these results, several in vivo studies found enhanced ROS formation in the brain after GSM RFR (1.6–6 W/kg) exposure with increased oxidative stress (Megha et al., 2015; Stefi et al., 2019; Zielinski et al., 2020). However, the level and extent of changes in oxidative stress parameters are specific to the dose and duration of exposure and the experimental setup. Megha et al. reported an increase in oxidative stress in the brains of male Fischer rats exposed to GSM modulated RFRs (900, 1800, 2100 MHz, for 60 days, SAR: 0.59, 0.58 and 0.66 mW/kg respectively) while shifting toward higher frequencies and SAR values (Megha et al., 2015). Taken together, the results of previous studies on this subject indicate that non-thermal RFR can be absorbed by particular charges, molecules, and cellular constructions; thus, they can stimulate important modulatory effects in living cells (Yakymenko et al., 2016). Kesari et al. reported that UMTS modulated RFR (2115 MHz, 2 h/day for 60 days SAR: 0.26 W/Kg) originating from 3 G technology caused DNA breaks in the brain of the Wistar rats (Kesari et al., 2014). On the other hand, Dasdag et al., who suggested that RFR is an environmental stress factor, determined that long-term exposure to GSM modulated 900 MHz RFR (2 h per day for 10 months, SAR: 0.17–0.58 W/kg) caused increases in the total antioxidant capacity and catalase level in the brain of the Wistar Albino rats (Dasdag et al., 2009). Şahin et al. observed an increase in oxidative DNA damage in the brain of the Wistar albino rats after 10 days of exposure to 3 G modulated 2100 MHz RFR (6 h per day, 5 consecutive days per week for 2 weeks, SAR: 0.4 W/kg), while they found a decrease in oxidative DNA damage after 40 days of application (Sahin et al., 2016). The reason for the emergence of these different results was said to be the adaptation of the body to long-term RFR exposure and the activation of DNA repair mechanisms (Sahin et al., 2016). In another study, Dasdag et al. stated that long-term exposure to Wi-Fi 2.4 GHz RFR (24 h a day for 12 months, SAR: 141.4 μW/kg and 7127 μW/kg) caused changes in miRNAs in the brain of the Wistar Albino rats, which could be associated with the prognosis of some brain diseases (Dasdag et al., 2015). Moreover, Dasdag et al. found in another study that exposure to GSM modulated 900 MHz RFR (2 h per day, 7 days a week for 10 months, SAR: 0.17–0.58 W/kg) increased the levels of beta-amyloid protein, protein carbonyl, and malondialdehyde in brains of Wistar Albino rats (Dasdag et al., 2012). On the other hand, Arendash et al. reported that RFR (GSM modulated, 918 MHz, 1 h/day, for 5 and 7 months, SAR: 0.25 W/kg) provided cognitive benefits by reducing the amount of amyloid beta in the brains of transgenic and non-transgenic mice with Alzheimer disease (Arendash et al., 2010). Sharma et al. reported that GSM 1800 MHz RFR (SAR: 0.433 W/kg)

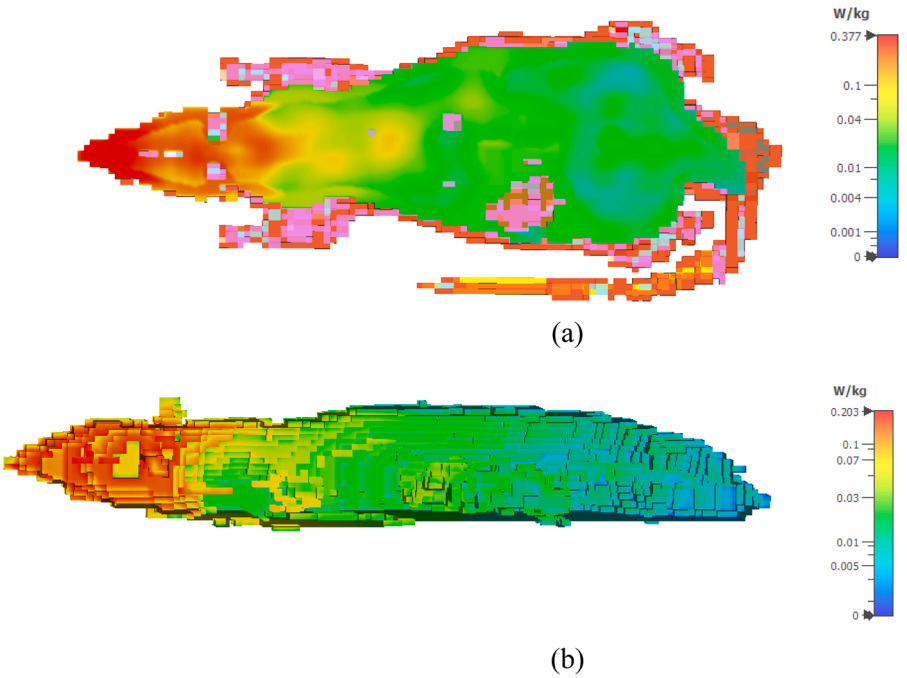


Fig. 3. SAR simulation results at 3500 MHz: a) 1 g average frontal plane, b) 10 g average sagittal plane.

Table 2
Ghrelin, nesfatin-1, irisin, TAS, TOS, and H_2O_2 in the brains of the rats.

	Healthy sham (Group 1)	Healthy + RFR (Group 2)	Diabetes sham (Group 3)	Diabetes + RFR (Group 4)	p
Ghrelin pg/mL	2967.7 ± 275.6^{ab}	3421.8 ± 214.9^{ac}	3327.6 ± 240.6^{a}	3841.5 ± 253.9^{d}	0.001
Nesfatin-1 ng/mL	1890.6 ± 221.9^{a}	1687.7 ± 190.5^{ab}	1684.3 ± 332.3^{ab}	1405.4 ± 255.1^{b}	0.018
Irisin ng/mL	31.2 ± 3.5^{a}	25.5 ± 3.5^{b}	14.8 ± 2.2^{c}	12.3 ± 0.7^{c}	0.001
TAS U/mL	10.5 ± 2.7^{a}	9.6 ± 2.4^{ab}	7.38 ± 0.98^{ac}	5.00 ± 0.4^{d}	0.002
TOS nmol/mL	0.23 ± 0.3^{a}	2.5 ± 0.5^{b}	3.719 ± 0.75^{b}	6.4 ± 1.2^{c}	<0.001
H_2O_2 ng/mL	378.2 ± 85.0^{a}	477.1 ± 57.3^{b}	726.259 ± 151.7^{c}	1068.5 ± 152.4^{d}	<0.001

$^{a,b,c,d:}$Different letters indicate significant differences between groups ($p < 0.05$).

caused an increase in oxidative stress and inflammatory cytokine release in the brains of Wistar rats (90 days at 4 h per day 5 days per week in a month) (Sharma et al., 2020). In another study, Sharma et al. used RFR at frequencies of 900, 1800, and 2100 MHz and SAR levels of 0.434 W/kg, 0.433 W/kg, and 0.453 W/kg, respectively. When animal exposure was limited to 1 h per day, 5 days/week for 1 month, a significant decrease in antioxidant enzyme capacity, increased ROS levels, and degraded pyramidal and Purkinje neurons were observed in the brains of the Wistar rats (Sharma et al., 2021). Similarly, Chauhan et al. revealed that RFR (2.45 GHz radiation source at 50 Hz modulation frequency) exposure (2 h per day for 35 day, SAR: 0.14 W/kg) caused histological and oxidative changes, reductions in pyramidal cells, and neuronal degradation in the brains of Wistar rats (Chauhan et al., 2017). Lai and Singh stated that acute 2-h exposure to 2450-MHz RFR (pulsed, 2μs pulse width, 500 pulses s^{-1} and continuous wave, SAR: 1.2 W/kg) can cause single and double chain breaks in the brain of Sprague Dawley rats due to oxidative stress (Lai and Singh, 1996). One of the major sources of ROS in cells is the mitochondrial electron transport chain, which can produce superoxide due to deteriorations in electron transport (Inoue et al., 2003). It was shown that formation of ROS by the mitochondrial pathway can be induced under GSM 1.8 GHz RFR exposure (SAR: from 0.4 W/kg to 27.5 W/kg) in human spermatozoa (De Iuliis et al., 2013). Taken together, the findings in the current literature on the biological effects of RFR convincingly demonstrate that exposure to low-intensity RFR causes the formation of substantial amounts of ROS in living cells and results in important oxidative stress (Yakymenko et al., 2016).

In our study, changes in the levels of nesfatin-1 and ghrelin, which are known as appetite hormones, were detected in the brains of rats exposed to RFR. More specifically, 5 G RFR caused a decrease in nesfatin levels and an increase in ghrelin levels in the brains of both diabetic and healthy rats. Recent studies have shown that nesfatin as an appetite suppressant (Shimizu and Mori, 2013) and ghrelin as an appetite stimulant (Morin et al., 2018) play active roles in adipose tissue accumulation and appetite mechanisms. That is, decreased nesfatin and increased ghrelin cause an increase in appetite. This indicates that exposure to 3.5 GHz RFR has an appetite-increasing effect on rats. Similarly, in a study in which they used RFR of a lower frequency, Tripathi et al. reported that RFR (2 h per day for 8 weeks, 1760 MHz, 0.3988 mW/cm^2, GSM, SAR: 0.181 W/kg) caused an increase in ghrelin levels in the brain of rats (Tripathi et al., 2021). It was stated that an increase in the amount of ghrelin causes an increase in appetite and thus the need for food (Tripathi et al., 2021). In addition, it was reported that in albino rats prolonged GSM 900 MHz RFR exposure (1 h/day, for 30 days, SAR: 0.9 W/kg) caused in an increase oxidative stress and apoptosis in the thyroid gland and a decrease plasma nesfatin-1 level (Hussien et al., 2020). In a recent study of 15 normal-weight young men aged 21–29 years, it was stated that exposure to GSM 900 MHz RFR emitted by two different mobile phone types (phone 1: Motorola L2 (Motorola Mobility LLC), Libertyville, IL, USA and phone 2: Nokia 5800d-1 (Nokia Group, Helsinki, Finland), SAR: 0.97 W/kg for phone 2 and 1.33 W/kg for phone 1) for 25 min per day significantly increased calorie and food intake (Wardzinski et al., 2022). On the other hand, Tang et al. reported that nesfatin-1 had antioxidative and antiapoptotic effects on the brain, thus being neuroprotective. It was also observed that nesfatin-1 had a significant effect on the suppression of brain damage caused by oxidative mechanisms (Tang et al., 2012). Studies showed that nesfatin-1 is a

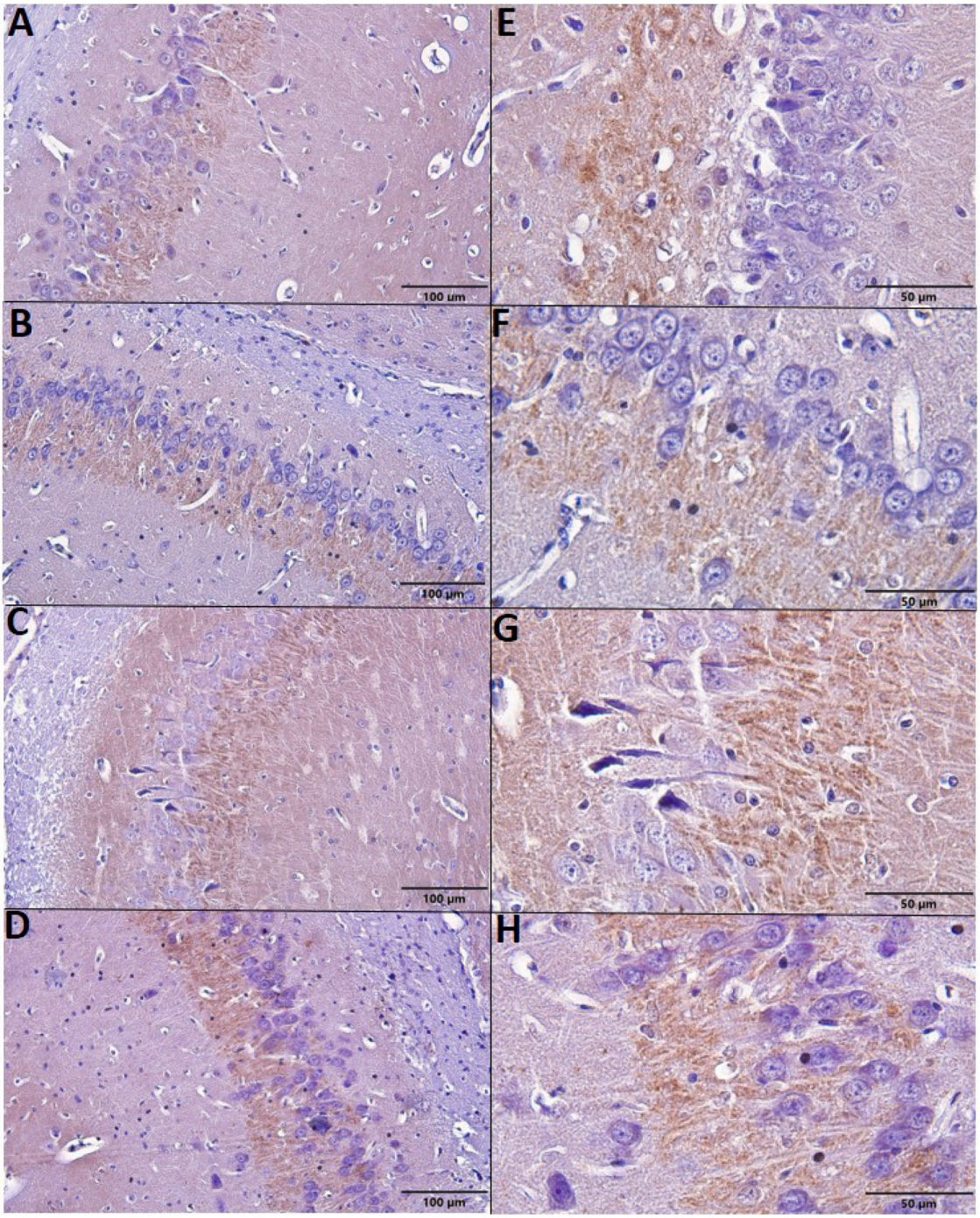


Fig. 4. Immunohistochemical images of anti-synaptophysin antibody in brain tissues of rats at 40 × and 100 × : A, E) Healthy sham (Group 1); B, F) Diabetes sham (Group 3); C, G) Healthy + 5 G (Group 2); D, H: Diabetes + 5 G (Group 4).

neuropeptide that plays an important role in stress responses and the pathology of mental and neurological disorders (Aydin et al., 2009; Könczöl et al., 2010; Pałasz et al., 2012). In addition, it was found that ghrelin promoted the formation of new brain cells and protected them from the effects of aging (Morgan et al., 2018). There is also evidence that ghrelin enhances perception. Animals fed low-calorie diets were shown to experience an increase in mental abilities, and ghrelin was thought to be effective in that. Mice injected with ghrelin had improved performance in learning and memory tests. The findings suggested that ghrelin increases the neural connections in the brain (Morgan et al., 2018).

In our study, a significant decrease in irisin level was detected in the brains of both diabetic and healthy rats exposed to RFR. Although irisin is a myokine secreted from skeletal muscles, it has major effects on various parts of the body, and particularly the central nervous system, impacting lipid metabolism, thermogenesis, browning of white adipose tissue, bone resorption, neuronal differentiation in the brain, and neuroprotection (Young et al., 2019). Moreover, it was stated that hippocampal neurogenesis is dose-dependently regulated by irisin (Moon et al., 2013). It was also reported that irisin expressed in the brain induces the expression of brain-derived neurotrophic factor in the rat hippocampus; thus, increased brain irisin levels can preserve memory. Moreover, it was shown in an Alzheimer rat model that an increase in irisin could prevent cognitive decline (Lourenco et al., 2019). On the

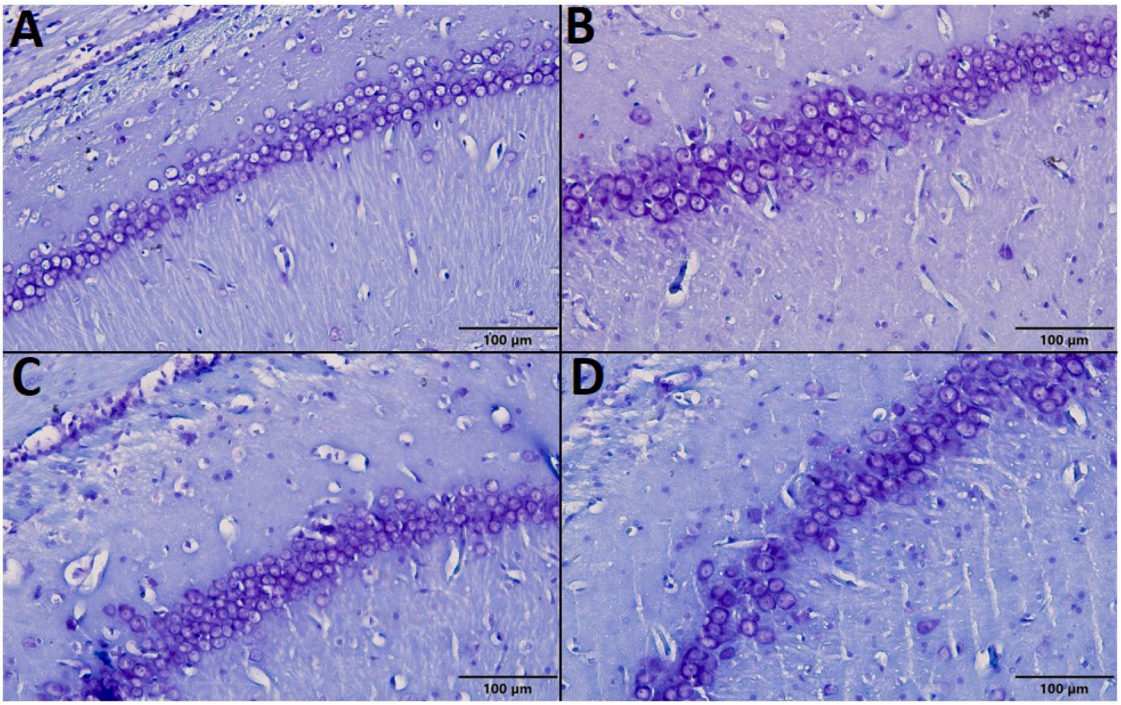


Fig. 5. Microscopic images of brain tissue stained with cresyl violet: A) Healthy sham (Group 1); B) Diabetes sham (Group 3), C) Healthy + 5 G (Group 2), D) Diabetes + 5 G (Group 4).

other hand, according to our results, as 5 G RFR causes a decrease in brain irisin levels, it can be thought that it may trigger neurodegenerative diseases such as Alzheimer disease.

According to our immunohistochemical results, no significant difference was observed between the groups in terms of synaptophysin (Fig. 1). Synaptophysin is a neuroendocrine tumor marker (Özaslan et al., 2014) and a synaptic protein involved in synaptic plasticity and cognitive function, and its amount is reduced in cases of synaptic degeneration induced by neuroinflammation (Yang et al., 2020; Zhou et al., 2020).

However, according to the cresyl violet staining results of the present study, the increase in degenerated neurons in the healthy and diabetic 5 G groups compared to the healthy and diabetic sham groups indicates that 3.5 GHz increases the number of degenerated neurons in the CA1 region of the hippocampus. This shows that long-term exposure to 3.5 GHz RFR may trigger dementia at later ages. It was also seen that 3.5 GHz RFR caused degeneration in the brain of healthy rats, and more intensely so in diabetic rats. Similarly, Hasan et al. performed cresyl violet staining in their study and reported that abnormally sized and shaped pyramidal cells were observed in the brains of mice exposed to RFR (4 G, 2400 MHz, 40–60 min/day for 60 days), and degenerated neurons were densely present (Hasan et al., 2022). There are many studies in the literature that provide evidence that RFR affects the central nervous system in the frequency range of 900–2400 MHz. It was reported that darkly stained granule cells in the DG areas of Wistar albino rats exposed to continuous modulated 900 MHz RFR (SAR: 2 W/kg) (Odaci et al., 2008), pyknotic neurons in the hippocampal CA region of Wistar albino rats exposed to 900 MHz RFR (Baş et al., 2013), and dark cytoplasm pyramidal neurons in the hippocampus of Sprague Dawley rats exposed to GSM 900 MHz RFR (SAR: 0.024 W/kg) (Şahin et al., 2015) were observed.

It was reported that GSM 900, 1800 MHz RFR exposure (for 60 min/5 days of the week during the one year SAR: from 8.6 to 93 mW/kg) increased the intracellular Ca^{2+} concentration and induced apoptosis in hippocampal and dorsal root ganglion neuron of Wistar rats (Ertilav et al., 2018). It is known that increased Ca^{2+} input will depolarize the inner mitochondrial membrane by increasing electron transport chain activity and ROS production (Bektas, 2021). Moreover, ROS may be involved in the actions of RFR emitted from wireless communication devices on biological systems (Ilhan et al., 2004; Nazıroğlu et al., 2012).

5. Conclusion

The data obtained in this study showed that 3.5 GHz RFR caused changes in energy metabolism and appetite in both diabetic and healthy rats. In addition, it was shown that 3.5 GHz can cause degenerative effects via oxidative damage in the brain. It was demonstrated that these effects may be more dangerous for diabetics according to the TAS, TOS, H_2O_2, ghrelin, nesfatin, and irisin levels and cresyl violet staining results. The results of this research reveal that 3.5 GHz RFR has the potential to alter nesfatin-1, irisin, and ghrelin levels. Further studies are needed.

Ethical statement

All experiments were performed in accordance with the guidelines provided by the Experimental Animal Laboratory and approved by the Animal Experiments Local Ethics Committee of Van Yuzuncu Yil University, Turkey (approval number: 2021/05-10). All experimental procedures were appropriate to the Guide for the Care and Use of Laboratory Animals of National Institutes of Health (NIH Publication No. 80-23; reformulated in 1996).

Author statement

All authors read and approved the final and revised manuscript. They warrant that the article is the authors' original work, has not received prior publication and is not under consideration for publication elsewhere.

Authors' contributions

HB and **SD** designed the study. **HB** and **SA** performed the in vivo study. **HB** and **SA** performed the biochemical analysis. **FA** performed the histopathology analysis. **KY** performed SAR simulation. **HB, SD** and **ZA** wrote the manuscript, **SD** supervised all the step of the study, All authors read and approved the final manuscript.

Conflict of interests

The authors have no conflict of interest.

Acknowledgements

This work was supported by Van Yuzuncu Yil University Scientific Research Foundation (BAP, Turkey, grant number: TYD-2021-9598). The authors would like to thank Dr. Mustafa Cakir and Yusuf Emir Bektaş for their valuable contribution.

References

Akdag, T., Odabas, F.O., 2020. Evaluation of serum levels of irisin and nesfatin-1 in patients with migraine without aura. Int J. Med. Biochem. 3, 67–72.
Algul, S., Ozcelik, O., Oto, G., Sarikaya, M., Goceroglu, R., Embiyaoglu, N., Caf, F., Öner, S., Akcan, A., 2021. Effects of curcumin administration on Nesfatin-1 levels in blood, brain and fat tissues of diabetic rats. Eur. Rev. Med. Pharmacol. Sci. 25, 1616–1621.
Alkis, M.E., Bilgin, H.M., Akpolat, V., Dasdag, S., Yegin, K., Yavas, M.C., Akdag, M.Z., 2019. Effect of 900-, 1800-, and 2100-MHz radiofrequency radiation on DNA and oxidative stress in brain. Electromagn. Biol. Med. 38, 32–47.
Altındağ, F., Rağbetli, M.Ç., Özdek, U., Koyun, N., Alhalboosi, J.K.I., Elasan, S., 2021. Combined treatment of sinapic acid and ellagic acid attenuates hyperglycemia in streptozotocin-induced diabetic rats. Food Chem. Toxicol. 156, 112443.
Arendash, G.W., Sanchez-Ramos, J., Mori, T., Mamcarz, M., Lin, X., Runfeldt, M., Wang, L., Zhang, G., Sava, V., Tan, J., 2010. Electromagnetic field treatment protects against and reverses cognitive impairment in Alzheimer's disease mice. J. Alzheimer's Dis. 19, 191–210.
Avci, B., Akar, A., Bilgici, B., Tunçel, Ö.K., 2012. Oxidative stress induced by 1.8 GHz radio frequency electromagnetic radiation and effects of garlic extract in rats. Int. J. Radiat. Biol. 88, 799–805.
Aydin, S., Dag, E., Ozkan, Y., Erman, F., Dagli, A.F., Kilic, N., Sahin, I., Karatas, F., Yoldas, T., Barim, A.O., 2009. Nesfatin-1 and ghrelin levels in serum and saliva of epileptic patients: hormonal changes can have a major effect on seizure disorders. Mol. Cell. Biochem. 328, 49–56.
Baş, O., Sönmez, O.F., Aslan, A., Ikinci, A., Hancı, H., Yıldırım, M., Kaya, H., Akça, M., Odacı, E., 2013. Pyramidal cell loss in the cornu ammonis of 32-day-old female rats following exposure to a 900 megahertz electromagnetic field during prenatal days 13–21. NeuroQuantology 11, 591–599.
Bathina, S., Das, U.N., 2021. Resolvin D1 decreases severity of streptozotocin-induced type 1 diabetes mellitus by enhancing BDNF levels, reducing oxidative stress, and suppressing inflammation. Int. J. Mol. Sci. 22, 1516.
Bektas, H., 2021. 5G and Health Concerns. Gece Publishing, Ankara.
Belpomme, D., Hardell, L., Belyaev, I., Burgio, E., Carpenter, D.O., 2018. Thermal and non-thermal health effects of low intensity non-ionizing radiation: an international perspective. Environ. Pollut. 242, 643–658.
Chauhan, P., Verma, H., Sisodia, R., Kesari, K.K., 2017. Microwave radiation (2.45 GHz)-induced oxidative stress: whole-body exposure effect on histopathology of Wistar rats. Electromagn. Biol. Med. 36, 20–30.
Chen, Y.B., Li, J., Liu, J.Y., Zeng, L.H., Wan, Y., Li, Y.R., Ren, D., Guo, G., 2011. Effect of electromagnetic pulses (EMP) on associative learning in mice and a preliminary study of mechanism. Int. J. Radiat. Biol. 87, 1147–1154.
Cummings, D.E., Purnell, J.Q., Frayo, R.S., Schmidova, K., Wisse, B.E., Weigle, D.S., 2001. preprandial rise in plasma ghrelin levels suggests a role in meal initiation in humans. Diabetes 50, 1714–1719.
Dasdag, S., Akdag, M.Z., 2016. The link between radiofrequencies emitted from wireless technologies and oxidative stress. J. Chem. Neuroanat. 75, 85–93.
Dasdag, S., Akdag, M.Z., Erdal, M.E., Erdal, N., Ay, O.I., Ay, M.E., Yilmaz, S.G., Tasdelen, B., Yegin, K., 2015. Effects of 2.4 GHz radiofrequency radiation emitted from Wi-Fi equipment on microRNA expression in brain tissue. Int. J. Radiat. Biol. 91, 555–561.
Dasdag, S., Akdag, M.Z., Kizil, G., Kizil, M., Cakir, D.U., Yokus, B., 2012. Effect of 900 MHz radio frequency radiation on beta amyloid protein, protein carbonyl, and malondialdehyde in the brain. Electromagn. Biol. Med. 31, 67–74.
Dasdag, S., Akdag, M.Z., Ulukaya, E., Uzunlar, A.K., Ocak, A.R., 2009. Effect of mobile phone exposure on apoptotic glial cells and status of oxidative stress in rat brain. Electromagn. Biol. Med. 28, 342–354.
Dasgupta, S., Wang, G.X., Simonich, M.T., Zhang, T.W., Truong, L., Liu, H.P., Tanguay, R. L., 2020. Impacts of high dose 3.5 GHz cellphone radiofrequency on zebrafish embryonic development. PLoS One 15.
De Iuliis, G.N., Newey, R.J., King, B.V., Aitken, R.J., 2013. Correction: mobile phone radiation induces reactive oxygen species production and DNA damage in human spermatozoa in vitro. PLoS One 8.
Dolan, M., Rowley, J., 2009. The precautionary principle in the context of mobile phone and base station radiofrequency exposures. Environ. Health Perspect. 117, 1329–1332.
Druce, M., Bloom, S.R., 2003. Central regulators of food intake. Curr. Opin. Clin. Nutr. Metab. Care 6, 361–367.
Ertilav, K., Uslusoy, F., Ataizi, S., Naziroglu, M., 2018. Long term exposure to cell phone frequencies (900 and 1800 MHz) induces apoptosis, mitochondrial oxidative stress and TRPV1 channel activation in the hippocampus and dorsal root ganglion of rats. Metab. Brain Dis. 33, 753–763.
Furman, B.L., 2015. Streptozotocin-induced diabetic models in mice and rats. Curr. Protoc. Pharmacol. 70, 5.47. 41–45.47. 20.
Hasan, I., Jahan, M.R., Islam, M.N., Islam, M.R., 2022. Effect of 2400 MHz mobile phone radiation exposure on the behavior and hippocampus morphology in Swiss mouse model. Saudi J. Biol. Sci. 29, 102–110.
Hussien, N.I., Mousa, A.M., Shoman, A.A., 2020. Decreased level of plasma nesfatin-1 in rats exposed to cell phone radiation is correlated with thyroid dysfunction, oxidative stress, and apoptosis. Arch. Physiol. Biochem. 1–7.
Ilhan, A., Gurel, A., Armutcu, F., Kamisli, S., Iraz, M., Akyol, O., Ozen, S., 2004. Ginkgo biloba prevents mobile phone-induced oxidative stress in rat brain. Clin. Chim. Acta 340, 153–162.
Inoue, M., Sato, E.F., Nishikawa, M., Park, A.-M., Kira, Y., Imada, I., Utsumi, K., 2003. Mitochondrial generation of reactive oxygen species and its role in aerobic life. Curr. Med. Chem. 10, 2495–2505.
Jego, S., Salvert, D., Renouard, L., Mori, M., Goutagny, R., Luppi, P.-H., Fort, P., 2012. Tuberal hypothalamic neurons secreting the satiety molecule Nesfatin-1 are critically involved in paradoxical (REM) sleep homeostasis. PLoS One 7, e52525.
Jin, L., Bo, X.M., 2021. Neuroprotection of sevoflurane against ischemia/reperfusion-induced brain injury through inhibiting GluN2A/GluN2B-PSD-95-MLK3 module. Exp. Brain Res. 239, 2701–2709.
Justin, A., Divakar, S., Ramanathan, M., 2018. Cerebral ischemia induced inflammatory response and altered glutaminergic function mediated through brain AT1 and not AT2 receptor. Biomed. Pharmacother. 102, 947–958.
Kamiş, N., Karabağ, F., 2019. Parasetamol İndüklü Hepatotoksisite Modelinde Kafeik Asit Fenil Ester'in İnflamasyon ve Oksidatif Stres Üzerine Etkisinin Araştırılması. Atatürk Üniversitesi Vet. Bilim. Derg. 14, 290–298.
Kesari, K.K., Kumar, S., Behari, J., 2011. 900-MHz microwave radiation promotes oxidation in rat brain. Electromagn. Biol. Med. 30, 219–234.
Kesari, K.K., Meena, R., Nirala, J., Kumar, J., Verma, H., 2014. Effect of 3G cell phone exposure with computer controlled 2-D stepper motor on non-thermal activation of the hsp27/p38MAPK stress pathway in rat brain. Cell Biochem. Biophys. 68, 347–358.
Kim, J.H., Chung, K.H., Hwang, Y.R., Park, H.R., Kim, H.J., Kim, H.-G., Kim, H.R., 2021. Exposure to RF-EMF alters postsynaptic structure and hinders neurite outgrowth in developing hippocampal neurons of early postnatal mice. Int. J. Mol. Sci. 22, 5340.
Kızılırmak, D., Bozkurt, B., Karamanlı, H., 2020. Relationship between ghrelin and obestatin levels and ghrelin/obestatin ratio in patients with asthma. Tuberk. ve Toraks 68, 9–16.
Könczöl, K., Bodnár, I., Zelena, D., Pintér, O., Papp, R.S., Palkovits, M., Nagy, G.M., Tóth, Z.E., 2010. Nesfatin-1/NUCB2 may participate in the activation of the hypothalamic–pituitary–adrenal axis in rats. Neurochem. Int. 57, 189–197.
Lai, H., Singh, N.P., 1996. Single- and double-strand DNA breaks in rat brain cells after acute exposure to radiofrequency electromagnetic radiation. Int. J. Radiat. Biol. 69, 513–521.
Lourenco, M.V., Frozza, R.L., de Freitas, G.B., Zhang, H., Kincheski, G.C., Ribeiro, F.C., Gonçalves, R.A., Clarke, J.R., Beckman, D., Staniszewski, A., 2019. Exercise-linked FNDC5/irisin rescues synaptic plasticity and memory defects in Alzheimer's models. Nat. Med. 25, 165–175.
Megha, K., Deshmukh, P.S., Banerjee, B.D., Tripathi, A.K., Ahmed, R., Abegaonkar, M.P., 2015. Low intensity microwave radiation induced oxidative stress, inflammatory response and DNA damage in rat brain. Neurotoxicology 51, 158–165.
Moon, H.-S., Dincer, F., Mantzoros, C.S., 2013. Pharmacological concentrations of irisin increase cell proliferation without influencing markers of neurite outgrowth and synaptogenesis in mouse H19-7 hippocampal cell lines. Metabolism 62, 1131–1136.
Moreno-Navarrete, J.M., Ortega, F., Serrano, M., Guerra, E., Pardo, G., Tinahones, F., Ricart, W., Fernández-Real, J.M., 2013. Irisin is expressed and produced by human muscle and adipose tissue in association with obesity and insulin resistance. J. Clin. Endocrinol. Metab. 98, E769–E778.
Morgan, A.H., Rees, D.J., Andrews, Z.B., Davies, J.S., 2018. Ghrelin mediated neuroprotection-A possible therapy for Parkinson's disease? Neuropharmacology 136, 317–326.
Morin, V., Hozer, F., Costemale-Lacoste, J.-F., 2018. The effects of ghrelin on sleep, appetite, and memory, and its possible role in depression: a review of the literature. L'Enceph. 44, 256–263.
Motawi, T.K., Darwish, H.A., Moustafa, Y.M., Labib, M.M., 2014. Biochemical modifications and neuronal damage in brain of young and adult rats after long-term exposure to mobile phone radiations. Cell Biochem. Biophys. 70, 845–855.
Nazıroğlu, M., Çelik, Ö., Özgül, C., Çiğ, B., Doğan, S., Bal, R., Gümral, N., Rodríguez, A., Pariente, J., 2012. Melatonin modulates wireless (2.45 GHz)-induced oxidative injury through TRPM2 and voltage gated Ca^{2+} channels in brain and dorsal root ganglion in rat. Physiol. Behav. 105, 683–692.
Odaci, E., Bas, O., Kaplan, S., 2008. Effects of prenatal exposure to a 900 MHz electromagnetic field on the dentate gyrus of rats: a stereological and histopathological study. Brain Res. 1238, 224–229.

Öntürk, H., Özbek, H., 2007. Carried out of experimental diabetes and the measurement of glycemic activity. Gen. Med. J. 17, 231–236.
Özaslan, E., Diri, H., Karaca, H., Şimşek, Y., Bayram, F., 2014. An Overview of Neuroendocrine Tumour Markers. Turk. J. Endocrinol. Metab. 18.
Pałasz, A., Krzystanek, M., Worthington, J., Czajkowska, B., Kostro, K., Wiaderkiewicz, R., Bajor, G., 2012. Nesfatin-1, a unique regulatory neuropeptide of the brain. Neuropeptides 46, 105–112.
Price, T.O., Samson, W.K., Niehoff, M.L., Banks, W.A., 2007. Permeability of the blood–brain barrier to a novel satiety molecule nesfatin-1. Peptides 28, 2372–2381.
Şahin, A., Aslan, A., Baş, O., İkinci, A., Özyılmaz, C., Sönmez, O.F., Çolakoğlu, S., Odacı, E., 2015. Deleterious impacts of a 900-MHz electromagnetic field on hippocampal pyramidal neurons of 8-week-old Sprague Dawley male rats. Brain Res. 1624, 232–238.
Sahin, D., Ozgur, E., Guler, G., Tomruk, A., Unlu, I., Sepici-Dinçel, A., Seyhan, N., 2016. The 2100 MHz radiofrequency radiation of a 3G-mobile phone and the DNA oxidative damage in brain. J. Chem. Neuroanat. 75, 94–98.
Sanders, A.P., Joines, W.T., Allis, J.W., 1985. Effects of continuous-wave, pulsed, and sinusoidal-amplitude-modulated microwaves on brain energy metabolism. Bioelectromagn. J. Bioelectromagn. Soc., Soc. Phys. Regul. Biol. Med. Eur. Bioelectromagn. Assoc. 6, 89–97.
Sharma, A., Shrivastava, S., Shukla, S., 2020. Exposure of radiofrequency electromagnetic radiation on biochemical and pathological alterations. Neurol. India 68, 1092.
Sharma, A., Shrivastava, S., Shukla, S., 2021. Oxidative damage in the liver and brain of the rats exposed to frequency-dependent radiofrequency electromagnetic exposure: biochemical and histopathological evidence. Free Radic. Res. 1–12.
Shehu, A., Mohammed, A., Magaji, R.A., Muhammad, M.S., 2016. Exposure to mobile phone electromagnetic field radiation, ringtone and vibration affects anxiety-like behaviour and oxidative stress biomarkers in albino wistar rats. Metab. Brain Dis. 31, 355–362.
Shimizu, H., Mori, M., 2013. Nesfatin-1: its role in the diagnosis and treatment of obesity and some psychiatric disorders. Calcium Bind. Proteins RAGE 327–338.
Singh, K.V., Gautam, R., Meena, R., Nirala, J.P., Jha, S.K., Rajamani, P., 2020. Effect of mobile phone radiation on oxidative stress, inflammatory response, and contextual fear memory in Wistar rat. Environ. Sci. Pollut. Res. 27, 19340–19351.
Stefi, A.L., Margaritis, L.H., Skouroliakou, A.S., Vassilacopoulou, D., 2019. Mobile phone electromagnetic radiation affects Amyloid Precursor Protein and α-synuclein metabolism in SH-SY5Y cells. Pathophysiology 26, 203–212.
Tan, S., Wang, H., Xu, X., Zhao, L., Zhang, J., Dong, J., Yao, B., Wang, H., Zhou, H., Gao, Y., 2017. Study on dose-dependent, frequency-dependent, and accumulative effects of 1.5 GHz and 2.856 GHz microwave on cognitive functions in Wistar rats. Sci. Rep. 7, 1–13.
Tang, C.-H., Fu, X.-J., Xu, X.-L., Wei, X.-J., Pan, H.-S., 2012. The anti-inflammatory and anti-apoptotic effects of nesfatin-1 in the traumatic rat brain. Peptides 36, 39–45.
Tóthová, B., Kovalská, M., Kalenská, D., Tomašcová, A., Lehotský, J., 2018. Histone hyperacetylation as a response to global brain ischemia associated with hyperhomocysteinemia in rats. Int. J. Mol. Sci. 19, 3147.
Tripathi, R., Banerjee, S.K., Nirala, J.P., Mathur, R., 2021. Simultaneous exposure to electromagnetic field from mobile phone and unimpeded fructose drinking during pre-, peri-, and post-pubertal stages perturbs the hypothalamic and hepatic regulation of energy homeostasis by early adulthood: experimental evidence. Environ. Sci. Pollut. Res. 1–14.
Tschop, M., Weyer, C., Tataranni, P.A., Devanarayan, V., Ravussin, E., Heiman, M.L., 2001. Circulating ghrelin levels are decreased in human obesity. Diabetes 50, 707–709.
Wang, Y., Jiang, Z., Zhang, L., Zhang, Z., Liao, Y., Cai, P., 2022. 3.5-GHz radiofrequency electromagnetic radiation promotes the development of Drosophila melanogaster. Environ. Pollut. 294, 118646.
Wang, Y.-h, Sun, C.-k, Li, X.-l, Huang, Y., Sun, J., 2018. Ghrelin attenuates ultraviolet B radiation-induced impairment in capacities of epidermal stem cells. Biomed. Pharmacother. 100, 36–41.
Wardzinski, E.K., Jauch-Chara, K., Haars, S., Melchert, U.H., Scholand-Engler, H.G., Oltmanns, K.M., 2022. Mobile phone radiation deflects brain energy homeostasis and prompts human food ingestion. Nutrients 14, 339.
Yakymenko, I., Tsybulin, O., Sidorik, E., Henshel, D., Kyrylenko, O., Kyrylenko, S., 2016. Oxidative mechanisms of biological activity of low-intensity radiofrequency radiation. Electromagn. Biol. Med. 35, 186–202.
Yang, L., Zhou, R., Tong, Y., Chen, P., Shen, Y., Miao, S., Liu, X., 2020. Neuroprotection by dihydrotestosterone in LPS-induced neuroinflammation. Neurobiol. Dis. 140, 104814.
Young, M.F., Valaris, S., Wrann, C.D., 2019. A role for FNDC5/Irisin in the beneficial effects of exercise on the brain and in neurodegenerative diseases. Prog. Cardiovasc. Dis. 62, 172–178.
Zhou, Y.-l, Yan, Y.-m, Li, S.-y, He, D.-h, Xiong, S., Wei, S.-f, Liu, W., Hu, L., Wang, Q., Pan, H.-f, 2020. 6-O-angeloylplenolin exerts neuroprotection against lipopolysaccharide-induced neuroinflammation in vitro and in vivo. Acta Pharmacol. Sin. 41, 10–21.
Zielinski, J., Ducray, A.D., Moeller, A.M., Murbach, M., Kuster, N., Mevissen, M., 2020. Effects of pulse-modulated radiofrequency magnetic field (RF-EMF) exposure on apoptosis, autophagy, oxidative stress and electron chain transport function in human neuroblastoma and murine microglial cells. Toxicol. Vitr. 68, 104963.